

Research Article: Confirmation | Neuronal Excitability

Electrophysiological properties of medium spiny neuron subtypes in the caudate-putamen of prepubertal male and female *Drd1a*-tdTomato line 6 BAC transgenic mice

Jaime A. Willett^{1,2,3}, Jinyan Cao^{1,2}, David M. Dorris¹, Ashlyn G. Johnson⁴, Laura A. Ginnari¹ and John Meitzen^{1,2,5,6}

¹Department of Biological Sciences, North Carolina State University, Raleigh, NC

²W.M. Keck Center for Behavioral Biology, North Carolina State University, Raleigh, NC

³Graduate Program in Physiology, North Carolina State University, Raleigh, NC

⁴Neuroscience Graduate Program, Emory University, Atlanta, GA

⁵Center for Human Health and the Environment, North Carolina State University, Raleigh, NC

⁶Comparative Medicine Institute, North Carolina State University, Raleigh, NC

<https://doi.org/10.1523/ENEURO.0016-19.2019>

Received: 14 January 2019

Revised: 12 February 2019

Accepted: 24 February 2019

Published: 7 March 2019

J.A.W., J.C., and J.M. designed research; J.A.W. and J.C. performed research; J.A.W., D.M.D., A.G.J., L.G., and J.M. analyzed data; J.A.W., D.M.D., and J.M. wrote the paper; J.M. contributed unpublished reagents/analytic tools.

Funding: <http://doi.org/10.13039/100000183DOD> | United States Army | RDECOM | Army Research Office (ARO)
W911NF-15-1-0476

Funding: <http://doi.org/10.13039/100000025HHS> | NIH | National Institute of Mental Health (NIMH)
R01MH109471

Funding: <http://doi.org/10.13039/100007703North Carolina State University> (NC State University)
Start-up Funds

Funding: <http://doi.org/10.13039/100000066HHS> | NIH | National Institute of Environmental Health Sciences (NIEHS)
P30ES025128

The authors declare no competing financial interests.

We acknowledge the following funding sources: Army Research Office STIR Award W911NF-15-1-0476, NIH R01MH109471 (JM), NC State University Start-up Funds (JM); and P30ES025128 (Center for Human Health and the Environment).

Corresponding author: John Meitzen at jemeitze@ncsu.edu

Cite as: eNeuro 2019; 10.1523/ENEURO.0016-19.2019

Alerts: Sign up at www.eneuro.org/alerts to receive customized email alerts when the fully formatted version of this article is published.

Accepted manuscripts are peer-reviewed but have not been through the copyediting, formatting, or proofreading process.

Copyright © 2019 Willett et al.

This is an open-access article distributed under the terms of the Creative Commons Attribution 4.0 International license, which permits unrestricted use, distribution and reproduction in any medium provided that the original work is properly attributed.

- 1 1. Title: **Electrophysiological properties of medium spiny neuron subtypes in the caudate-**
2 **putamen of prepubertal male and female *Drd1a*-tdTomato line 6 BAC transgenic mice**
- 3 2. Abbreviated title: Caudate-putamen MSN subtype electrophysiology
- 4 3. Author names and affiliations: Jaime A. Willett^{1,2,3}, Jinyan Cao^{1,2}, David M. Dorris¹, Ashlyn
5 G. Johnson⁴, Laura A. Ginnari¹, John Meitzen^{1,2,5,6} 1. Department of Biological Sciences, North
6 Carolina State University, Raleigh, NC; 2. W.M. Keck Center for Behavioral Biology, North
7 Carolina State University, Raleigh, NC; 3. Graduate Program in Physiology, North Carolina
8 State University, Raleigh, NC; 4. Neuroscience Graduate Program, Emory University, Atlanta,
9 GA; 5. Center for Human Health and the Environment, North Carolina State University, Raleigh,
10 NC; 6. Comparative Medicine Institute, North Carolina State University, Raleigh, NC
- 11 4. Corresponding author: John Meitzen, Dept. Biological Sciences, NC State University, Campus
12 Box 7617, David Clark Labs room 166, Raleigh, NC 27695-7617, jmeitze@ncsu.edu
- 13 5. Number of figures, tables, multimedia (separately): 5, 2, 0
- 14 6. Number of words for abstract, introduction, and discussion (separately): 232, 644, 1536
- 15 7. Acknowledgements: We thank Stephanie Proaño and Dr. Amanda Krentzel for their technical
16 support, and Drs. Jonathan Ting, David Aylor, Heather Patisaul, and Scott Belcher for advice
17 regarding mice selection and breeding.
- 18 8. Conflicts of Interest: The authors declare no competing financial interests.
- 19 9. Funding sources: We acknowledge the following funding sources: Army Research Office
20 STIR Award W911NF-15-1-0476, NIH R01MH109471 (JM), NC State University Start-up
21 Funds (JM); and P30ES025128 (Center for Human Health and the Environment).

22

23 Abstract

24 The caudate-putamen is a striatal brain region essential for sensorimotor behaviors, habit
25 learning, and other cognitive and premotor functions. The output and predominant neuron of the
26 caudate-putamen is the medium spiny neuron (MSN). MSNs present discrete cellular subtypes
27 that show differences in neurochemistry, dopamine receptor expression, efferent targets, gene
28 expression, functional roles, and most importantly for this study, electrophysiological properties.
29 MSN subtypes include the striatonigral and the striatopallidal groups. Most studies identify the
30 striatopallidal MSN subtype as being more excitable than the striatonigral MSN subtype.
31 However, there is some divergence between studies regarding the exact differences in
32 electrophysiological properties. Furthermore, MSN subtype electrophysiological properties have
33 not been reported disaggregated by biological sex. We addressed these questions using
34 prepubertal male and female *Drd1a*-tdTomato line 6 BAC transgenic mice, an important
35 transgenic line that has not yet received extensive electrophysiological analysis. We made acute
36 caudate-putamen brain slices and assessed a robust battery of 16 relevant electrophysiological
37 properties using whole-cell patch clamp recording, including intrinsic membrane, action
38 potential, and miniature excitatory postsynaptic current (mEPSC) properties. We found that: (1)
39 MSN subtypes exhibited multiple differential electrophysiological properties in both sexes,
40 including rheobase, action potential threshold and width, input resistance in both the linear and
41 rectified ranges, and mEPSC amplitude; (2) select electrophysiological properties showed
42 interactions between MSN subtype and sex. These findings provide a comprehensive evaluation
43 of mouse caudate-putamen MSN subtype electrophysiological properties across females and
44 males, both confirming and extending previous studies.

45 Significance Statement

46 The findings presented here provide the most comprehensive evaluation of the
47 electrophysiological properties of caudate-putamen medium spiny neuron (MSN) subtypes ever
48 performed in a single study, both in terms of electrophysiological metrics and animal sex. These
49 data selectively confirm, diverge from, and extend the findings of previous studies, providing a
50 firm foundation upon which to pursue future studies of caudate-putamen MSNs.

51

52 Introduction

53 The most abundant neuron type in the mammalian caudate-putamen is the medium spiny neuron
54 (MSN), also called the spiny projection neuron (Graveland and Difiglia, 1985; Gerfen and
55 Surmeier, 2011). The MSN is the output neuron of the caudate-putamen and other striatal brain
56 regions, and is implicated in a wide range of cognitive and sensorimotor behaviors and relevant
57 striatal disorders (Kreitzer and Malenka, 2008; Koob and Volkow, 2010; Maia and Frank, 2011).
58 In order to regulate these behaviors, MSNs integrate glutamatergic, dopaminergic, GABAergic,
59 cholinergic, estrogenic, and other inputs to influence both internal and external targets. MSNs are
60 phenotypically diverse, encompassing at least two different subtypes, which differ in
61 neurochemistry, dopamine receptor expression, efferent targets, gene expression, functional
62 roles, and electrophysiological properties (Gerfen et al., 1990; Cepeda et al., 2008; Gertler et al.,
63 2008; Shuen et al., 2008; Ade et al., 2011; Kramer et al., 2011; Kreitzer and Berke, 2011; Chan
64 et al., 2012; Kravitz et al., 2012; Ma et al., 2012; Ma et al., 2013; Planert et al., 2013; Fieblinger
65 et al., 2014; Friend and Kravitz, 2014; Keeler et al., 2014; Gokce et al., 2016; Schier et al., 2017;
66 Sebel et al., 2017; Ho et al., 2018).

67 These two MSN subtypes include the striatonigral and the striatopallidal. Striatonigral MSNs
68 express D1 dopamine receptors, which are the product of the gene *Drd1a*, and contain the
69 neuropeptides substance P and dynorphin. Striatopallidal MSNs express D2 dopamine receptors,
70 which are the product of the gene *Drd2*, and contain the neuropeptide enkephalin. Previous
71 studies exploring caudate-putamen MSN subtype-specific electrophysiological properties have
72 generally identified the *Drd2*-expressing subtype as being more excitable compared to the
73 *Drd1a*-expressing subtype. However, there is some divergence between studies regarding the
74 exact differences in electrophysiological properties (Table 1), and few studies have
75 comprehensively evaluated a wide variety of cellular electrophysiological properties in
76 individual MSNs of identified subtypes. Furthermore, all previous studies of caudate-putamen
77 MSN subtypes have been performed in rats or mice of either solely male or unreported sex,
78 typical of the majority of neuroscience pre-clinical studies (Beery and Zucker, 2011; Shansky
79 and Woolley, 2016; Will et al., 2017). This is problematic given that striatal-mediated behaviors
80 and disorders exhibit sex differences and/or sex steroid hormone sensitivity in phenotype and/or
81 incidence (Calhoun, 1962; Eckel et al., 2000; Zurkovsky et al., 2007; Hosseini-Kamkar and

82 Morton, 2014; Yoest et al., 2018), and that striatal region and developmental stage-influenced
 83 sex differences exist in MSN electrophysiological properties, at least in rats (Arnauld et al.,
 84 1981; Tansey et al., 1983; Mermelstein et al., 1996; Wissman et al., 2011; Dorris et al., 2015;
 85 Tozzi et al., 2015; Cao et al., 2016; Willett et al., 2016; Cao et al., 2018; Proano et al., 2018).

86 To address these gaps in knowledge, we employed female and male B6 *Cg-Tg (Drd1a-*
 87 *tdTomato)* line 6 Calak/J hemizygous mice, a bacterial artificial chromosome (BAC) transgenic
 88 mouse line initially developed in the laboratory of Dr. Nicole Calakos (Ade et al., 2011). This
 89 mouse line and many others are widely used for experiments targeting neuronal subtypes
 90 (Valjent et al., 2009; Ting and Feng, 2014). An advantage of this particular BAC transgenic line
 91 is that it expresses a sensitive and specific fluorescent reporter for the *Drd1a*-expressing MSN
 92 subtype, enabling accurate identification of MSNs subtypes within a single mouse. Other
 93 advantages of this mouse line compared to other candidates are that this line exhibits normal
 94 caudate-putamen-mediated behaviors and does not appear to show obvious cellular or physical
 95 confounds (Ade et al., 2011; Enoksson et al., 2012; Thibault et al., 2013). We made acute brain
 96 slices of male and female mouse caudate-putamen and then recorded individual MSN subtypes
 97 using whole-cell patch clamp. We analyzed a comprehensive battery of caudate-putamen MSN
 98 subtype electrophysiological attributes to test the hypothesis that MSN electrophysiological
 99 properties differs by subtype across both males and females, including action potential,
 100 excitability, passive membrane and input resistance properties, and miniature excitatory synaptic
 101 currents (mEPSCs).

102

103 **Materials**

104 Animals

105 Male B6 *Cg-Tg (Drd1a-tdTomato)* line 6 Calak/J mice and female C57BL/6 background mice
 106 were purchased from the Jackson Laboratory (JAX stock number 16204). During the first week
 107 after arrival mice were individually housed. After the first week mice were housed in male and
 108 female pairs to enable breeding of hemizygous offspring. Offspring aged post-natal day (PND)
 109 17-22 from F1 litters were used in experiments (n=25) and were matched between experimental
 110 groups (10 *Drd1a* male mice: PND 19.4 ± 0.2 ; 7 *Drd1a* female mice: PND 21.0 ± 0.2 ; 4 *Drd2*
 111 male mice: PND 19.8 ± 0.5 ; 3 *Drd2* female mice: PND 20.0 ± 0.7 ; $P > 0.05$). Approximately 3

neurons were recorded from each mouse. Mice were not weaned before experimental use and female vaginal opening had not occurred before experimental use. Pups were ear punched for identification and genotyping. Mice were housed in a temperature- and light-controlled room ($22 \pm 1^\circ\text{C}$, 40-45% humidity, 12:12-hour light/dark cycle, lights on at 7:00 AM). All cages were washed polysulfone bisphenol A free and were filled with bedding manufactured from virgin hardwood chips (Beta Chip, NEPCO, Warrensburg, NY) to avoid the endocrine disruptors present in corncob bedding (Markaverich et al., 2002; Mani et al., 2005; Villalon Landeros et al., 2012). Soy protein-free rodent chow (2020X; Teklad) and glass-bottle provided water were available *ad libitum*. All animals in these studies were maintained according to the applicable portions of the Animal Welfare Act and the U.S. Department of Health and Human Services *Guide for the Care and Use of Laboratory Animals*, and the study was approved by the Institutional Animal Care and Use Committee.

Animal Genotyping

Mice genotyping was performed by Celplor (Raleigh, NC), using the following primers according to the Jackson Laboratory suggested protocol: Transgene Forward (forward primer, 12153, 5-CTT CTG AGG CGG AAA GAA CC-3), Transgene Reverse (reverse primer, 12154, 5-TTT CTG ATT GAG AGC ATT CG-3), PCR product length is 750 base pairs. The internal control was: Internal Positive Control Forward (oIMR7338) CTA GGC CAC AGA ATT GAA AGA TCT, Internal Positive Control Reverse (oIMR7339) GTA GGT GGA AAT TCT AGC ATC ATC C), PCR product length is 324 base pairs. PCR was performed according to the suggested protocol from Jackson Laboratory: 1 cycle of 94°C for 2 min, 5 cycles of 94°C for 30 sec, $60\text{--}55^\circ\text{C}$ touchdown ramp for 30 sec and 72°C for 30 sec, 25 cycles of 94°C for 30 sec, 55°C for 30 sec and 72°C for 30 sec, followed by 1 cycle of 72°C for 5 min.

Acute Brain Slice Preparation

Brain slices for electrophysiological recordings were prepared following a previously published protocol (Dorris et al., 2014). Briefly, mice were deeply anesthetized with isoflurane gas and killed by decapitation. The brain was then dissected rapidly into ice-cold, oxygenated sucrose artificial cerebellum spinal fluid (s-ACSF) containing (in mM): 75 sucrose, 1.25 NaH_2PO_4 , 3 MgCl_2 , 0.5 CaCl_2 , 2.4 Na pyruvate, 1.3 ascorbic acid from Sigma-Aldrich, St. Louis, MO, and 75 NaCl, 25 NaHCO_3 , 15 dextrose, 2 KCl from Fisher, Pittsburg, PA. The osmolarity of the s-

142 ACSF was between 295-305 mOsm, and pH was between 7.2-7.4. Coronal brain slices (300 μ m)
 143 were prepared using a vibratome and then incubated in regular ACSF containing (in mM): 126
 144 NaCl, 26 NaHCO₃, 10 dextrose, 3 KCl, 1.25 NaH₂PO₄, 1 MgCl₂, 2 CaCl₂ (295-305 mOsm, pH
 145 7.2-7.4) for 30 minutes at 30 \pm 1 $^{\circ}$ C, and then at least 30 minutes at room temperature (21-23 $^{\circ}$ C).
 146 Slices were stored submerged in room temperature, oxygenated ACSF for up to 5 hours after
 147 sectioning in a large volume bath holder.

148 Electrophysiological Recording

149 Slices were allowed to rest at least 1 hour after sectioning, and were then placed in a Zeiss
 150 Axioscope equipped with IR-DIC and fluorescent optics, a Dage IR-1000 video camera, and 10X
 151 and 40X lenses with optical zoom. Slices were superfused with oxygenated ACSF heated to 28 \pm
 152 0.2 $^{\circ}$ C. Whole-cell patch-clamp recordings were used to record the electrical properties of
 153 fluorescently labeled Drd1a and unlabeled Drd2 MSNs in the caudate-putamen (Figure 1).
 154 Caudate-putamen gross regional volume and cell density and soma size do not grossly vary by
 155 sex in rodents and humans (Meitzen et al., 2011; Wong et al., 2016). Glass patch electrodes
 156 contained the following solution (in mM): 115 K D-gluconate, 8 NaCl, 2 EGTA, 2 MgCl₂, 2
 157 MgATP, 0.3 NaGTP, 10 phosphocreatine from Sigma-Aldrich and 10 HEPES from Fisher (285
 158 mOsm, pH 7.2-7.4). Signals were amplified, filtered (2 kHz), and digitized (10 kHz) with a
 159 MultiClamp 700B amplifier attached to a Digidata 1550 system and a personal computer using
 160 pClamp 10 software. Membrane potentials were corrected for a calculated liquid junction
 161 potential of -13.5 mV. Using previously described procedures (Dorris et al., 2015), recordings
 162 were first made in current clamp to assess neuronal action potential and passive membrane
 163 properties. MSNs were identified by their medium-sized somas, the presence of a slow ramping
 164 subthreshold depolarization in response to low-magnitude positive current injections, a
 165 hyperpolarized resting membrane potential more negative than -65 mV, inward rectification, and
 166 prominent spike after hyperpolarization (O'Donnell and Grace, 1993; Belleau and Warren, 2000).
 167 After MSN identification and current clamp recording, oxygenated ACSF containing both the
 168 GABA_A receptor antagonist Picrotoxin (PTX, 150 μ M; Fisher) and the voltage-gated sodium
 169 channel blocker tetrodotoxin (TTX, 1 μ M, Abcam Biochemicals) was applied to the bath solution
 170 to abolish GABAergic inhibitory post-synaptic current events and action potentials, respectively.
 171 Following an established protocol (Cao et al., 2016), once depolarizing current injection no
 172 longer generated an action potential after exposure to TTX and PTX, MSNs were voltage

173 clamped at -70 mV and miniature excitatory post-synaptic currents (mEPSCs) were recorded for
174 at least five minutes. In all experiments input/series resistance was monitored for changes and
175 cells were excluded if resistance changed more than 25%.

176 Data Analysis

177 Intrinsic electrophysiological properties, action potential and mEPSC characteristics were
178 recorded and analyzed using pClamp 10. After break-in, the resting membrane potential was first
179 allowed to stabilize for ~1-2 minutes, as in (Mu et al., 2010). Then, at least three series of
180 depolarizing and hyperpolarizing current injections were applied to elicit basic
181 neurophysiological properties. The electrophysiological properties measured followed previously
182 described definitions (Dorris et al., 2015; Cao et al., 2016; Willett et al., 2016; Willett et al.,
183 2018), which were based upon those of Perkel and colleagues (Farries and Perkel, 2000; Farries
184 and Perkel, 2002; Farries et al., 2005; Meitzen et al., 2009). For each neuron, measurements were
185 made of at least three action potentials generated from the minimum current injection necessary
186 to elicit one or two action potentials. These measurements were then averaged to generate the
187 reported action potential measurements for that neuron. For action potential measurements, only
188 the first generated action potential was analyzed. Action potential threshold was defined as the
189 first point of sustained positive acceleration of voltage ($\delta^2V/\delta t^2$) that was also more than three
190 times the SD of membrane noise before the detected threshold (Baufreton et al., 2005). The slope
191 of the linear range of the evoked firing rate to positive current curve (FI slope) was calculated
192 from the first current stimulus which evoked an action potential to the first current stimulus that
193 generated an evoked firing rate that persisted for at least two consecutive current stimuli. Input
194 resistance in the linear, non-rectified range was calculated from the steady-state membrane
195 potential in response to -0.02 nA hyperpolarizing injected current. Rectified range input
196 resistance, inward rectification, and percent inward rectification ($RRIR/IR \times 100$) was calculated
197 using the most hyperpolarizing current injected into the MSN, as previously described (Belleau
198 and Warren, 2000). The membrane time constant was calculated by fitting a single exponential
199 curve to the membrane potential change in response to -0.02 nA hyperpolarizing pulses.
200 mEPSCs frequency, amplitude, and decay were analyzed off-line using Mini Analysis
201 (Synaptosoft, <http://www.synaptosoft.com/MiniAnalysis/>). Threshold was set as 5 pA, noise
202 filter was set at 1000 Hz, and accurate event detection was validated by visual inspection.

203 Statistics

204 Experiments were analyzed via a two-way ANOVA with a Tukey's multiple comparisons post-
 205 hoc test (Excel version 2010; Microsoft, Redmond, WA; Prism version 6.07, GraphPad
 206 Software, La Jolla, CA). P values < 0.05 were considered *a priori* as significant. Values 6
 207 standard deviations away from the mean were *a priori* excluded from analysis. Effect size was
 208 assessed using Cohen's *d* value (Calin-Jageman, 2018). *d* values are reported numerically and
 209 were classified *a priori* as small (>0.20), medium (>0.50) and large (>0.80) (Cohen, 1977). Data
 210 are presented as mean ± standard error of the mean (SEM).

212 **Results**

213 A total of 86 MSNs from the caudate-putamen of male and female B6 *Cg-Tg (Drd1a-tdTomato)*
 214 6 Calak/J hemizygous mice were recorded for this study. Recorded MSNs were *a priori* sorted
 215 into four experimental groups: male tdTomato-labeled *Drd1a*-positive MSNs, female tdTomato-
 216 labeled *Drd1a*-positive MSNs, male tdTomato-unlabeled MSNs, and female tdTomato-unlabeled
 217 MSNs. MSNs unlabeled by tdTomato fluorescence nearly exclusively comprise the *Drd2*-
 218 positive MSN subtype, including during the developmental age and striatal region assessed in
 219 this study (Ade et al., 2011; Enoksson et al., 2012; Thibault et al., 2013). tdTomato-unlabeled
 220 MSNs have rare (~1.6%) contamination with *Drd1a*-positive MSNs. Thus, for convenience in
 221 this study we refer to all tdTomato-unlabeled MSNs as *Drd2* MSNs, with the full
 222 acknowledgment that this designation is putative.

223 Action potential properties

224 To test the hypothesis that action potential properties differed across MSN subtype and animal
 225 sex, MSNs were current-clamped and injected with increasing amounts of depolarizing current to
 226 elicit action potential generation (Figure 2A). The resting membrane potential, rheobase, action
 227 potential threshold, width, amplitude, action potential afterhyperpolarization peak amplitude and
 228 time to afterhyperpolarization peak amplitude were assessed (Table 2). MSNs exhibited
 229 differences between subtypes or interactions between subtype and sex in several attributes,
 230 including the resting membrane potential (Figure 2B). Compared between groups, the resting
 231 membrane potential of male *Drd1a* MSNs was hyperpolarized compared to male *Drd2* MSNs
 232 ($P < 0.01$; $d = 0.86$), but not between female *Drd1a* MSNs compared to female *Drd2* MSNs

233 ($P > 0.05$, $d = 0.42$). Rheobase, or the minimum current sufficient for eliciting action potential
 234 generation, was increased in Drd1a MSNs compared to Drd2 MSNs (Figure 2C). Compared
 235 between groups, the rheobase of male Drd1a MSNs differed from male and female Drd2 MSNs
 236 ($P < 0.05$, $d = 0.74$; $P < 0.05$, $d = 0.77$; respectively). The action potential threshold was
 237 hyperpolarized in Drd1a MSNs compared to Drd2 MSNs (Figure 2D). Compared between
 238 groups, the action potential threshold of female Drd1a MSNs differed from female Drd2 MSNs
 239 ($P < 0.01$, $d = 1.00$), but not between male Drd1a MSNs and male Drd2 MSNs ($P > 0.05$, $d = 0.05$).
 240 The action potential width of Drd1a MSNs was longer compared to Drd2 MSNs (Figure 2E).
 241 Compared between groups, the action potential width of male Drd1a MSNs was increased
 242 compared to male Drd2 MSNs ($P < 0.01$, $d = 1.24$), but not between female Drd1a MSNs and
 243 female Drd2 MSNs ($P > 0.05$, $d = 0.03$). Considering other passive properties, no differences were
 244 detected between MSN subtype or sex in action potential amplitude, action potential
 245 afterhyperpolarization peak amplitude and time to afterhyperpolarization peak amplitude (Table
 246 2). These differences in action potential properties indicate that Drd1a MSNs are less likely to
 247 generate an action potential at low magnitudes of injected depolarizing current than are Drd2
 248 MSNs.

249 Intrinsic excitability and action potential generation rates

250 These differences between MSN subtype rheobase, action potential threshold, width, and time to
 251 first action potential properties indicate that overall MSN excitability may also differ by subtype
 252 (Figure 3A). To assess this, we began by analyzing the frequency of action potentials evoked by
 253 depolarizing current injections. Action potential firing rates evoked by depolarizing current
 254 injections were visibly decreased in Drd1a compared to Drd2 MSNs in both males and females
 255 (Figure 3B). To further probe the relationship between MSN subtype and action potential
 256 generation, we quantified the slope of the evoked firing rate to positive current curve (FI slope).
 257 FI slope differed by subtype but not sex, with Drd1a MSNs exhibiting decreased excitability
 258 compared to Drd2 MSNs (Figure 3C). Compared between groups, the FI slope of male Drd1a
 259 MSNs differed from male Drd2 MSNs ($P < 0.01$, $d = 0.96$). Female Drd1A MSNs differed from
 260 male Drd2 MSNs ($P < 0.0001$, $d = 1.25$) and female Drd2 MSNs ($P < 0.05$, $d = 1.10$). These data
 261 indicate that excitability robustly differs between MSN subtypes.

262 Passive membrane properties

263 To test the hypothesis that MSN passive electrophysiological properties differed by subtype and
 264 sex, a series of increasingly negative current pulses were injected into individual neurons (Figure
 265 4A). MSN subtypes exhibited differences in input resistance across both the linear and rectified
 266 ranges (Figure 4B). Input resistance in the linear and rectified ranges, % inward rectification, the
 267 time constant of the membrane, and capacitance were analyzed (Table 2). Linear range input
 268 resistance was largely decreased in Drd1a MSNs compared to Drd2 MSNs (Figure 4C).
 269 Compared between groups, the linear range input resistance of male Drd1a MSNs differed from
 270 male Drd2 MSNs ($P < 0.05$, $d = 0.67$), but did not differ between female Drd1a MSNs and female
 271 Drd2 MSNs ($P > 0.05$, $d = 0.34$). Male Drd2 MSNs also differed from female Drd1a MSNs
 272 ($P < 0.05$, $d = 0.83$). Rectified range input resistance did not differ between MSN subtypes (Figure
 273 4D) or other measures of inward rectification (Table 2). Considering other passive properties, no
 274 differences were detected between MSN subtype or sex in the time constant of the membrane,
 275 and capacitance (Table 2). Collectively, these analyses indicate that input resistance varies
 276 between MSN subtypes, with no differences in other passive membrane properties.

277 mEPSC properties

278 We voltage-clamped 18 male and 17 female Drd1a MSNs and 10 male and 6 female Drd2 MSNs
 279 at -70 mV and recorded mEPSCs in the presence of TTX and PTX (Figure 5A). mEPSC
 280 frequency, amplitude and decay were analyzed (Table 2). mEPSC amplitude was increased in
 281 Drd1a MSNs compared to Drd2 MSNs (Figure 5B). Compared between groups, the mEPSC
 282 amplitude of male Drd1a MSNs differed from female Drd2 MSNs ($P < 0.01$, $d = 0.82$) but not male
 283 Drd2 MSNs ($P > 0.05$, $d = 0.67$). The mEPSC amplitude of female Drd1a MSNs differed from
 284 female Drd2 MSNs ($P < 0.001$, $d = 1.74$). mEPSC decay did not differ between MSN subtype or
 285 sex (Figure 5C). Likewise, mEPSC frequency did not differ between MSN subtype or sex
 286 (Figure 5D). These data indicate that mEPSC amplitude differs between MSN subtypes.

287

288 **Discussion**

289 MSNs form at least two major pathways depending on their dopaminergic receptor and
 290 neuropeptide expression, electrophysiological properties, where they project, and ultimately their
 291 effect on behavior. The caudate-putamen MSNs of the direct pathway predominantly express
 292 D1-dopamine receptors, contain substance P and dynorphin, project to the basal ganglia output

nuclei, and stimulate downstream behavioral output. Indirect pathway MSNs express D2-dopamine receptors, contain enkephalin, project to the lateral globus pallidus, and leads to inhibition of downstream behavioral output. This study comprehensively evaluates mouse caudate-putamen MSN subtype electrophysiological properties, extending previous studies that targeted a smaller battery of electrical properties and that were performed solely in males or mice of unknown sex (Table 1). Electrophysiological properties differed between MSN subtypes, with Drd2 MSNs exhibiting increased intrinsic excitability compared to Drd1a MSNs, indicated most notably by differences in rheobase, action potential threshold, input resistance in the linear range, and increased FI Slope. Interestingly, this robust set of properties exhibits varying degrees of consistence with previous literature on MSN subtype electrophysiology, and select electrophysiological properties showed statistical interactions between subtype and biological sex.

The detected increase in excitability in Drd2 MSNs is generally consistent with previous studies of MSN subtypes in rodents across striatal regions, although there are subtle differences depending on the assessed electrophysiological metric and perhaps age (Onn et al., 1994; Onn et al., 1994; Onn et al., 1994; Venance and Glowinski, 2003; Kreitzer and Malenka, 2007; Ade et al., 2008; Cepeda et al., 2008; Gertler et al., 2008; Chan et al., 2012; Ma et al., 2012; Planert et al., 2013; Reig and Silberberg, 2014; Maurice et al., 2015; Cao et al., 2018; Goodliffe et al., 2018). Perhaps the most consistent metric indicating increased excitability in Drd2 MSNs compared to Drd1a MSNs is the decreased rheobase in Drd2 MSNs. Every study that has assessed this property has detected this difference, despite utilizing varying protocols and electrophysiological methods. From an electrophysiological perspective, differences in rheobase are rarely the sole electrophysiological difference between neuron types. Generally, a shift in rheobase is accompanied by concomitant changes in properties such as resting membrane potential, input resistance in the linear range, and/or action potential threshold. For instance, Gertler and colleagues detected changes in rheobase accompanied by changes in resting membrane potential and input resistance, but not action potential threshold (Gertler et al., 2008). Planert and colleagues detected changes in rheobase accompanied by a change in input resistance, but not action potential threshold or resting membrane potential in rats but not mice (Planert et al., 2013). Cepeda and colleagues did not assess rheobase, but did detect a difference in action potential threshold (Cepeda et al., 2008). The current study detected a difference in

324 rheobase accompanied by changes in action potential threshold and input resistance, supporting a
 325 model where the decreased rheobase values in Drd2 MSN subtypes is largely driven by a
 326 hyperpolarized action potential threshold and an increased input resistance. The increase in
 327 excitability observed in Drd2 MSNs could ultimately translate to a decrease in behavioral output.
 328 However, this particular interpretation is highly tentative given that MSNs make complex
 329 calculations between dopamine, glutamate, intrinsic properties, and other neuromodulators.
 330 Interestingly, we detected an interaction between MSN subtype and sex in resting membrane
 331 potential and action potential threshold. Thus, it is possible that the reason why the results of our
 332 study differ from those of Gertler and colleagues is because of the use of animals of
 333 undetermined sex in that study.

334 Regarding excitatory synaptic input, the current study detected an increase mEPSC amplitude in
 335 Drd2 MSN subtypes compared to Drd1a MSN subtypes. To our knowledge, this is the first
 336 indication that mEPSC amplitude can differ by MSN subtype (Table 1). This may be due to a
 337 variance and power interaction, although previous studies of MSN subtypes employed similar
 338 experimental N. This finding does align with previous research which detected large amplitude
 339 AMPA-mediated synaptic events in Drd2 MSNs that were not seen in Drd1a MSNs (Cepeda et
 340 al., 2008). The recording conditions under which the mEPSCs were assessed in this study
 341 eliminate non-AMPA-mediated currents (Proano et al., 2018). A number of factors could
 342 potentially mediate this difference in mEPSC amplitude, including morphological differences
 343 and/or differences in AMPA receptor number or subunit composition (Tallaksen-Greene and
 344 Albin, 1996; Vorobjev et al., 2000). Supporting this, there is evidence that the size of
 345 corticostriatal presynaptic terminals is larger on Drd2 MSN spines compared to Drd1a MSN
 346 spines (Lei et al., 2004). One possibility why previous studies did not detect a significant
 347 difference in mEPSC amplitude is because the effect size for this particular attribute is larger in
 348 females compared to males. Previous studies either only tested males or did not report sex, or
 349 sex-specific findings. Following this, two previous studies detected a greater sEPSC and mEPSC
 350 frequency in caudate putamen Drd2 MSNs compared to Drd1a MSNs that is not accompanied by
 351 differences in amplitude or decay (Kreitzer and Malenka, 2007; Cepeda et al., 2008). However,
 352 this literature is mixed as Cepeda and colleagues detected a difference in mEPSC rise time, and
 353 Day et al. did not detect a difference in mEPSC frequency in prepubertal animals, and Goodliffe
 354 et al. did not detect a difference in mEPSC frequency in adult animals (Day et al., 2006; Cepeda

et al., 2008; Goodliffe et al., 2018). It is possible that this variability in findings is in some part explained by the neglect or overrepresentation of one sex compared to another.

There are other factors which may also play a role, including animal age. Most studies of MSN subtype properties used mice that were between P17 and P30 (Table 1). During these periods, various levels of MSN synaptic maturation are occurring, which could contribute to variance in mEPSC properties (Tepper et al., 1998; Uryu et al., 1999). Gertler and colleagues employed a wide variety of ages to demonstrate that MSN subtype intrinsic properties differ before puberty, but the study did not assess excitatory synaptic properties (Gertler et al., 2008). Goodliffe and colleagues assessed at a much older age (~P365), and found differences in intrinsic properties but not mEPSC properties (Table 1). Thus, our assessment of the literature is that there is ample evidence for differences in MSN subtype electrophysiological properties prepuberty, but that there is a real need for further studies in adult animals, especially within the context of excitatory synapse properties, sex-specific hormone dynamics, and animal sex, especially since the current study is the only available analysis by sex in mouse caudate-putamen.

Similarly, Drd1a and Drd2 MSN subtypes display different sensitivities to neuromodulators such as dopamine during prepubertal development (Lieberman et al., 2018). Indeed, it has been documented in multiple striatal regions that dopamine receptor expression and/or action shows sex-specific effects during puberty (Andersen et al., 1997; Andersen et al., 2002; Kopec et al., 2018). Interestingly, excitatory currents generated by pyramidal tract stimulation show an increased amplitude in Drd1a MSNs compared to Drd2 MSNs in adult male and female mice that were not analyzed with regard to sex (Kress et al., 2013). In *in vivo* experiments in adult female mice, Drd1a MSNs were found to be more responsive to excitatory glutamatergic input compared to Drd2 MSNs (Escande et al., 2016). However, this study employed the line 5 Drd1a-tdTomato BAC-transgenic mice, which express properties such as an X-linked inheritance pattern and undefined mammary glands that reduces this strain's utility for assessing interactions between MSN subtypes and sex (Shuen et al., 2008; Ade et al., 2011). Subtype-specific differences in the development of glutamatergic and dopaminergic inputs onto MSNs in the caudate-putamen require further research, especially in the context of biological sex, environmental stimuli, and animals beyond mice.

384 The strain and/or species is also a relevant factor in explaining differences in MSN subtype
 385 electrophysiological properties across studies. For instance, multiple strains of transgenic mice
 386 have been employed across studies which have employed a variety of means to determine MSN
 387 subtype identity. Cepeda et al., Gertler et al., and the current study all targeted *Drd1a* or *Drd2*
 388 expression to identify MSN subtypes (albeit with different transgenic strategies), whereas other
 389 studies have employed different targets such as the muscarinic M4 receptor locus which labels
 390 striatonigral MSNs (Kreitzer and Malenka, 2007). There is some evidence that there is
 391 incomplete overlap between M4 and *Drd1a* dopamine receptors which may contribute to
 392 variance in detected electrophysiological properties, including sEPSC frequency between M4
 393 and D1 cells (Bernard et al., 1992; Cepeda et al., 2008). Here we employed the B6 *Cg-Tg*
 394 (*Drd1a*-tdTomato) 6 Calak/J hemizygous mice (line 6). We chose this strain because of its
 395 established high specificity, in that tdTomato-labeled MSNs almost exclusively consist of *Drd1a*
 396 MSNs, and that tdTomato-unlabeled MSNs exhibit only ~1.6% contamination with *Drd1a* MSNs
 397 (Ade et al., 2011; Enoksson et al., 2012; Thibault et al., 2013). Furthermore, the tdTomato label
 398 is easily detected using standard fluorescent microscopy, optimizing differentiation for whole-
 399 cell patch clamp. While the line 6 version of this transgenic mouse line does not show the
 400 obvious confounds for sex research that the line 5 version displays, including the X-linked
 401 inheritance pattern and undefined mammary glands, caution is always necessary with any
 402 transgenic mouse line that targets dopamine receptors. It is possible that transgenes targeting
 403 dopamine receptors subtly disrupt sexual differentiation, especially given the long documented
 404 and recently re-affirmed sex differences and hormone-sensitivity of the dopaminergic system in
 405 both rats and mice (Di Paolo, 1994; Becker, 1999; Calipari et al., 2017). Independent of sex,
 406 other mouse lines with transgenic manipulations of the dopamine system by attaching
 407 fluorophores have shown aberrant striatal-mediated behaviors, especially when strain and genetic
 408 homozygosity were not carefully monitored (Kramer et al., 2011; Chan et al., 2012). We raise
 409 this possibility neither to argue that transgenic mice in general are not useful for neuroscience
 410 research nor for understanding the effects of sex and steroid sex hormones. Several mouse
 411 models have made critical contributions to our understanding of sexual differentiation, most
 412 notably the four core genotypes (De Vries et al., 2002), including as applied to the caudate-
 413 putamen (Chen et al., 2009). Rather, we argue that the specific disadvantages and advantages of
 414 each research animal should be thoughtfully considered, especially for studies of the impact of

415 natural variables such as sex upon individual neuron function. There is no “one size fits all”
 416 mouse strain, just as there is no “one size fits all” strain of rat or any other research animal,
 417 echoing arguments presented by many investigators in diverse contexts (Beach, 1950; Krebs,
 418 1975; Young et al., 2013; Brenowitz and Zakon, 2015; Ellenbroek and Yoon, 2016; Klinck et al.,
 419 2017; Remage-Healey et al., 2017). Regarding species differences, to our knowledge, there is
 420 only one study which has assessed MSN subtype electrophysiological properties in the caudate
 421 putamen of a species other than mice. Similar to the current study in mice, Planert and colleagues
 422 found a difference in rheobase and related properties in prepubertal rats of unreported sex
 423 (Planert et al., 2013). Synaptic properties were not assessed.

424 Further complicating interpretation was the number of interactions between MSN subtype and
 425 sex detected by the current study. Given that animals were assessed before pubertal onset but
 426 after the perinatal critical period for hormone-induced organization of the neural substrate, it is
 427 possible that these sex differences were generated through some combination of
 428 masculinizing/defeminizing hormone action, genes, or epigenetics. All three of these
 429 mechanisms are potentially at work in the caudate-putamen and could contribute to the MSN
 430 subtype and sex interactions observed here (Chen et al., 2009; Cao et al., 2016). Previous studies
 431 in mice employed only males, animals of unreported sex, or animals of both sex sexes that were
 432 pooled for data analysis. This lack of consideration of biological sex is problematic given the
 433 long-known sex differences in striatal mediated behaviors, disorders, MSN properties, and
 434 neuromodulator systems such as dopamine (Mermelstein et al., 1996; McLean and Anderson,
 435 2009; Carroll and Anker, 2010; Young and Korszun, 2010; Becker and Chartoff, 2018; Meitzen
 436 et al., 2018). While this work has predominantly been performed in rats, importantly, adult mice
 437 exhibit sex differences in striatal gene expression and function in both the caudate putamen and
 438 nucleus accumbens (Chen et al., 2009; Calipari et al., 2017). The current study detected an
 439 interaction in action potential threshold, which was also found to differ by sex in prepubertal rats
 440 (Dorris et al., 2015). Other electrophysiological properties also differed by sex in rats, including
 441 the frequency of evoked action potentials to injected current and the action potential
 442 afterhyperpolarization, but were not found to differ by the current study in mice. This difference
 443 between mice and rats may be due to a number of potential factors, including but not limited to
 444 variance between inbred and outbred rodent strains, overall species differences and the effects of
 445 domestication, MSN subtype sampling bias, developmental trajectory, environmental factors

446 such as stress, and/or location within the caudate-putamen or striatum as a whole. For a
447 phylogenetically ancient and highly conserved brain region such as the caudate-putamen, it will
448 be particularly interesting to investigate the intersecting roles of subtype, development, and
449 biological sex in influencing MSN electrophysiological properties across a wide range of animals
450 with divergent reproductive behaviors.

451 **References**

- 452 Ade KK, Janssen MJ, Ortinski PI, Vicini S (2008) Differential tonic GABA conductances in
 453 striatal medium spiny neurons. *J Neurosci* 28: 1185-1197.
- 454 Ade KK, Wan Y, Chen M, Gloss B, Calakos N (2011) An Improved BAC Transgenic
 455 Fluorescent Reporter Line for Sensitive and Specific Identification of Striatonigral
 456 Medium Spiny Neurons. *Front Syst Neurosci* 5: 32.
- 457 Andersen SL, Rutstein M, Benzo JM, Hostetter JC, Teicher MH (1997) Sex differences in
 458 dopamine receptor overproduction and elimination. *Neuroreport*. 8: 1495-1498.
- 459 Andersen SL, Thompson AP, Krenzel E, Teicher MH (2002) Pubertal changes in gonadal
 460 hormones do not underlie adolescent dopamine receptor overproduction.
 461 *Psychoneuroendocrinology* 27: 683-691.
- 462 Arnault E, Dufy B, Pestre M, Vincent JD (1981) Effects of estrogens on the responses of
 463 caudate neurons to microiontophoretically applied dopamine. *Neurosci Lett* 21: 325-331.
- 464 Baufreton J, Atherton JF, Surmeier DJ, Bevan MD (2005) Enhancement of excitatory synaptic
 465 integration by GABAergic inhibition in the subthalamic nucleus. *J Neurosci* 25: 8505-
 466 8517.
- 467 Beach FA (1950) The snark was a boojum. *Am Psychol*: 115-124.
- 468 Becker JB (1999) Gender differences in dopaminergic function in striatum and nucleus
 469 accumbens. *Pharmacol Biochem Behav*. 64: 803-812.
- 470 Becker JB, Chartoff E (2018) Sex differences in neural mechanisms mediating reward and
 471 addiction. *Neuropsychopharmacology*: [Epub ahead of print].
- 472 Beery AK, Zucker I (2011) Sex bias in neuroscience and biomedical research. *Neurosci*
 473 *Biobehav Rev* 35: 565-572.
- 474 Belleau ML, Warren RA (2000) Postnatal development of electrophysiological properties of
 475 nucleus accumbens neurons. *J Neurophysiol* 84: 2204-2216.
- 476 Bernard V, Normand E, Bloch B (1992) Phenotypical characterization of the rat striatal neurons
 477 expressing muscarinic receptor genes. *J Neurosci* 12: 3591-3600.
- 478 Brenowitz EA, Zakon HH (2015) Emerging from the bottleneck: benefits of the comparative
 479 approach to modern neuroscience. *Trends Neurosci* 38: 273-278.
- 480 Calhoun JC (1962). The ecology and sociology of the Norway Rat, U.S. Department of Health,
 481 Education, and Welfare, PHS NO. 1008.
- 482 Calin-Jageman R (2018) The New Statistics for Neuroscience Majors: Thinking in Effect Sizes.
 483 *The Journal of Undergraduate Neuroscience Education* 16: E21-E25.
- 484 Calipari ES, Juarez B, Morel C, Walker DM, Cahill ME, Ribeiro E, Roman-Ortiz C,
 485 Ramakrishnan C, Deisseroth K, Han MH, Nestler EJ (2017) Dopaminergic dynamics
 486 underlying sex-specific cocaine reward. *Nat Commun* 8: 13877.
- 487 Cao J, Dorris DM, Meitzen J (2016) Neonatal masculinization blocks increased excitatory
 488 synaptic input in female rat nucleus accumbens core. *Endocrinology* 157: 3181-3196.
- 489 Cao J, Dorris DM, Meitzen J (2018) Electrophysiological properties of medium spiny neurons in
 490 the nucleus accumbens core of prepubertal male and female *Drd1a*-tdTomato line 6 BAC
 491 transgenic mice. *J Neurophysiol* 120: 1712-1727.
- 492 Carroll ME, Anker JJ (2010) Sex differences and ovarian hormones in animal models of drug
 493 dependence. *Horm Behav* 58: 44-56.
- 494 Cepeda C, Andre VM, Yamazaki I, Wu N, Kleiman-Weiner M, Levine MS (2008) Differential
 495 electrophysiological properties of dopamine D1 and D2 receptor-containing striatal
 496 medium-sized spiny neurons. *Eur J Neurosci* 27: 671-682.

- 497 Chan CS, Peterson JD, Gertler TS, Glajch KE, Quintana RE, Cui Q, Sebel LE, Plotkin JL, Shen
498 W, Heiman M, Heintz N, Greengard P, Surmeier DJ (2012) Strain-specific regulation of
499 striatal phenotype in Drd2-eGFP BAC transgenic mice. *J Neurosci* 32: 9124-9132.
- 500 Chen X, Grisham W, Arnold AP (2009) X chromosome number causes sex differences in gene
501 expression in adult mouse striatum. *Eur J Neurosci*. 29: 768-776.
- 502 Cohen J (1977). Statistical power analysis for the behavioral sciences (Rev. ed.). Hillsdale, NJ,
503 USA, Lawrence Erlbaum Associates, Inc.
- 504 Day M, Wang Z, Ding J, An X, Ingham CA, Shering AF, Wokosin D, Ilijic E, Sun Z, Sampson
505 AR, Mugnaini E, Deutch AY, Sesack SR, Arbuthnott GW, Surmeier DJ (2006) Selective
506 elimination of glutamatergic synapses on striatopallidal neurons in Parkinson disease
507 models. *Nat Neurosci* 9: 251-259.
- 508 De Vries GJ, Rissman EF, Simerly RB, Yang LY, Scordalakes EM, Auger CJ, Swain A, Lovell-
509 Badge R, Burgoyne PS, Arnold AP (2002) A model system for study of sex chromosome
510 effects on sexually dimorphic neural and behavioral traits. *J Neurosci*. 22: 9005-9014.
- 511 Di Paolo T (1994) Modulation of brain dopamine transmission by sex steroids. *Rev Neurosci*. 5:
512 27-41.
- 513 Dorris DM, Cao J, Willett JA, Hauser CA, Meitzen J (2015) Intrinsic excitability varies by sex in
514 pre-pubertal striatal medium spiny neurons. *J Neurophysiol* 113: 720-729.
- 515 Dorris DM, Hauser CA, Minnehan CE, Meitzen J (2014) An aerator for brain slice experiments
516 in individual cell culture plate wells. *J Neurosci Methods* 238: 1-10.
- 517 Eckel LA, Houpt TA, Geary N (2000) Spontaneous meal patterns in female rats with and without
518 access to running wheels. *Physiol Behav* 70: 397-405.
- 519 Ellenbroek B, Youn J (2016) Rodent models in neuroscience research: is it a rat race? *Dis Model*
520 *Mech* 9: 1079-1087.
- 521 Enoksson T, Bertran-Gonzalez J, Christie MJ (2012) Nucleus accumbens D2- and D1-receptor
522 expressing medium spiny neurons are selectively activated by morphine withdrawal and
523 acute morphine, respectively. *Neuropharmacology* 62: 2463-2471.
- 524 Escande MV, Taravini IR, Zold CL, Belforte JE, Murer MG (2016) Loss of Homeostasis in the
525 Direct Pathway in a Mouse Model of Asymptomatic Parkinson's Disease. *J Neurosci* 36:
526 5686-5698.
- 527 Farries MA, Meitzen J, Perkel DJ (2005) Electrophysiological properties of neurons in the basal
528 ganglia of the domestic chick: conservation and divergence in the evolution of the avian
529 basal ganglia. *Journal of neurophysiology* 94: 454-467.
- 530 Farries MA, Perkel DJ (2000) Electrophysiological properties of avian basal ganglia neurons
531 recorded in vitro. *Journal of neurophysiology* 84: 2502-2513.
- 532 Farries MA, Perkel DJ (2002) A telencephalic nucleus essential for song learning contains
533 neurons with physiological characteristics of both striatum and globus pallidus. *J*
534 *Neurosci* 22: 3776-3787.
- 535 Fieblinger T, Graves SM, Sebel LE, Alcacer C, Plotkin JL, Gertler TS, Chan CS, Heiman M,
536 Greengard P, Cenci MA, Surmeier DJ (2014) Cell type-specific plasticity of striatal
537 projection neurons in parkinsonism and L-DOPA-induced dyskinesia. *Nat Commun* 5:
538 5316.
- 539 Friend DM, Kravitz AV (2014) Working together: basal ganglia pathways in action selection.
540 *Trends Neurosci* 37: 301-303.

- 541 Gerfen CR, Engber TM, Mahan LC, Susel Z, Chase TN, Monsma FJ, Jr., Sibley DR (1990) D1
542 and D2 dopamine receptor-regulated gene expression of striatonigral and striatopallidal
543 neurons. *Science* 250: 1429-1432.
- 544 Gertler TS, Chan CS, Surmeier DJ (2008) Dichotomous anatomical properties of adult striatal
545 medium spiny neurons. *J Neurosci* 28: 10814-10824.
- 546 Gokce O, Stanley GM, Treutlein B, Neff NF, Camp JG, Malenka RC, Rothwell PE, Fuccillo
547 MV, Sudhof TC, Quake SR (2016) Cellular Taxonomy of the Mouse Striatum as
548 Revealed by Single-Cell RNA-Seq. *Cell Reports* 16: 1126-1137.
- 549 Goodliffe JW, Song H, Rubakovic A, Chang W, Medalla M, Weaver CM, Luebke JI (2018)
550 Differential changes to D1 and D2 medium spiny neurons in the 12-month-old Q175+/-
551 mouse model of Huntington's Disease. *PLoS One* 13: e0200626.
- 552 Ho H, Both M, Siniard A, Sharma S, Notwell JH, Wallace M, Leone DP, Nguyen A, Zhao E,
553 Lee H, Zwilling D, Thompson KR, Braithwaite SP, Huentelman M, Portmann T (2018) A
554 Guide to Single-Cell Transcriptomics in Adult Rodent Brain: The Medium Spiny Neuron
555 Transcriptome Revisited. *Front Cell Neurosci* 12: 159.
- 556 Hosseini-Kamkar N, Morton JB (2014) Sex differences in self-regulation: an evolutionary
557 perspective. *Front Neurosci* 8: 233.
- 558 Keeler JF, Pretsell DO, Robbins TW (2014) Functional implications of dopamine D1 vs. D2
559 receptors: A 'prepare and select' model of the striatal direct vs. indirect pathways.
560 *Neuroscience* 282: 156-175.
- 561 Klinck MP, Mogil JS, Moreau M, Lascelles BDX, Flecknell PA, Poitte T, Troncy E (2017)
562 Translational pain assessment: could natural animal models be the missing link? *Pain*
563 158: 1633-1646.
- 564 Koob GF, Volkow ND (2010) Neurocircuitry of addiction. *Neuropsychopharmacology*. 35: 217-
565 238. Epub .
- 566 Kopec AM, Smith CJ, Ayre NR, Sweat SC, Bilbo SD (2018) Microglial dopamine receptor
567 elimination defines sex-specific nucleus accumbens development and social behavior in
568 adolescent rats. *Nat Commun* 9: 3769.
- 569 Kramer PF, Christensen CH, Hazelwood LA, Dobi A, Bock R, Sibley DR, Mateo Y, Alvarez VA
570 (2011) Dopamine D2 receptor overexpression alters behavior and physiology in *Drd2*-
571 *EGFP* mice. *J Neurosci* 31: 126-132.
- 572 Kravitz AV, Tye LD, Kreitzer AC (2012) Distinct roles for direct and indirect pathway striatal
573 neurons in reinforcement. *Nat Neurosci* 15: 816-818.
- 574 Krebs HA (1975) The August Krogh Principle: "For many problems there is an animal on which
575 it can be most conveniently studied". *J Exp Zool* 194: 221-226.
- 576 Kreitzer AC, Berke JD (2011) Investigating striatal function through cell-type-specific
577 manipulations. *Neuroscience* 198: 19-26.
- 578 Kreitzer AC, Malenka RC (2007) Endocannabinoid-mediated rescue of striatal LTD and motor
579 deficits in Parkinson's disease models. *Nature* 445: 643-647.
- 580 Kreitzer AC, Malenka RC (2008) Striatal plasticity and basal ganglia circuit function. *Neuron*
581 60: 543-554.
- 582 Kress GJ, Yamawaki N, Wokosin DL, Wickersham IR, Shepherd GM, Surmeier DJ (2013)
583 Convergent cortical innervation of striatal projection neurons. *Nat Neurosci* 16: 665-667.
- 584 Lei W, Jiao Y, Del Mar N, Reiner A (2004) Evidence for differential cortical input to direct
585 pathway versus indirect pathway striatal projection neurons in rats. *J Neurosci* 24: 8289-
586 8299.

- 587 Lieberman OJ, McGuirt AF, Mosharov EV, Pigulevskiy I, Hobson BD, Choi S, Frier MD,
588 Santini E, Borgkvist A, Sulzer D (2018) Dopamine Triggers the Maturation of Striatal
589 Spiny Projection Neuron Excitability during a Critical Period. *Neuron* 99: 540-554 e544.
- 590 Ma YY, Cepeda C, Chatta P, Franklin L, Evans CJ, Levine MS (2012) Regional and cell-type-
591 specific effects of DAMGO on striatal D1 and D2 dopamine receptor-expressing
592 medium-sized spiny neurons. *ASN Neuro* 4: pii: e00077.
- 593 Ma YY, Henley SM, Toll J, Jentsch JD, Evans CJ, Levine MS, Cepeda C (2013) Drug-primed
594 reinstatement of cocaine seeking in mice: increased excitability of medium-sized spiny
595 neurons in the nucleus accumbens. *ASN Neuro* 5: 257-271.
- 596 Maia TV, Frank MJ (2011) From reinforcement learning models to psychiatric and neurological
597 disorders. *Nat Neurosci* 14: 154-162.
- 598 Mani SK, Reyna AM, Alejandro MA, Crowley J, Markaverich BM (2005) Disruption of male
599 sexual behavior in rats by tetrahydrofurandiols (THF-diols). *Steroids* 70: 750-754.
- 600 Markaverich B, Mani S, Alejandro MA, Mitchell A, Markaverich D, Brown T, Velez-Trippe C,
601 Murchison C, O'Malley B, Faith R (2002) A novel endocrine-disrupting agent in corn
602 with mitogenic activity in human breast and prostatic cancer cells. *Environ Health*
603 *Perspect* 110: 169-177.
- 604 Maurice N, Liberge M, Jaouen F, Ztaou S, Hanini M, Camon J, Deisseroth K, Amalric M,
605 Kerkerian-Le Goff L, Beurrier C (2015) Striatal Cholinergic Interneurons Control Motor
606 Behavior and Basal Ganglia Function in Experimental Parkinsonism. *Cell Rep* 13: 657-
607 666.
- 608 McLean CP, Anderson ER (2009) Brave men and timid women? A review of the gender
609 differences in fear and anxiety. *Clin Psychol Rev* 29: 496-505.
- 610 Meitzen J, Meisel RL, Mermelstein PG (2018) Sex Differences and the Effects of Estradiol on
611 Striatal Function. *Curr Opin Behav Sci* 23: 42-48.
- 612 Meitzen J, Pflepsen KR, Stern CM, Meisel RL, Mermelstein PG (2011) Measurements of neuron
613 soma size and density in rat dorsal striatum, nucleus accumbens core and nucleus
614 accumbens shell: differences between striatal region and brain hemisphere, but not sex.
615 *Neurosci Lett* 487: 177-181.
- 616 Meitzen J, Weaver AL, Brenowitz EA, Perkel DJ (2009) Plastic and stable electrophysiological
617 properties of adult avian forebrain song-control neurons across changing breeding
618 conditions. *J Neurosci.* 29: 6558-6567.
- 619 Mermelstein PG, Becker JB, Surmeier DJ (1996) Estradiol reduces calcium currents in rat
620 neostriatal neurons via a membrane receptor. *J Neurosci.* 16: 595-604.
- 621 Mu P, Moyer JT, Ishikawa M, Zhang Y, Panksepp J, Sorg BA, Schluter OM, Dong Y (2010)
622 Exposure to cocaine dynamically regulates the intrinsic membrane excitability of nucleus
623 accumbens neurons. *J Neurosci* 30: 3689-3699.
- 624 O'Donnell P, Grace AA (1993) Physiological and morphological properties of accumbens core
625 and shell neurons recorded in vitro. *Synapse* 13: 135-160.
- 626 Onn SP, Berger TW, Grace AA (1994) Identification and characterization of striatal cell
627 subtypes using in vivo intracellular recording and dye-labeling in rats: III. Morphological
628 correlates and compartmental localization. *Synapse* 16: 231-254.
- 629 Onn SP, Berger TW, Grace AA (1994) Identification and characterization of striatal cell
630 subtypes using in vivo intracellular recording in rats: I. Basic physiology and response to
631 corticostriatal fiber stimulation. *Synapse* 16: 161-180.

- 632 Onn SP, Berger TW, Grace AA (1994) Identification and characterization of striatal cell
633 subtypes using in vivo intracellular recording in rats: II. Membrane factors underlying
634 paired-pulse response profiles. *Synapse* 16: 195-210.
- 635 Planert H, Berger TK, Silberberg G (2013) Membrane properties of striatal direct and indirect
636 pathway neurons in mouse and rat slices and their modulation by dopamine. *PLoS One* 8:
637 e57054.
- 638 Proano S, Morris HJ, Kunz LM, Dorris DM, Meitzen J (2018) Estrous cycle-induced sex
639 differences in medium spiny neuron excitatory synaptic transmission and intrinsic
640 excitability in adult rat nucleus accumbens core. *J Neurophysiol* 120: 1356-1373.
- 641 Reig R, Silberberg G (2014) Multisensory integration in the mouse striatum. *Neuron* 83: 1200-
642 1212.
- 643 Remage-Healey L, Krentzel AA, Macedo-Lima M, Vahaba D (2017) Species Diversity Matters
644 in Biological Research. *Policy Insights from the Behavioral and Brain Sciences* 4: 210-
645 218.
- 646 Schier CJ, Marks WD, Paris JJ, Barbour AJ, McLane VD, Maragos WF, McQuiston AR, Knapp
647 PE, Hauser KF (2017) Selective Vulnerability of Striatal D2 versus D1 Dopamine
648 Receptor-Expressing Medium Spiny Neurons in HIV-1 Tat Transgenic Male Mice. *J*
649 *Neurosci* 37: 5758-5769.
- 650 Sebel LE, Graves SM, Chan CS, Surmeier DJ (2017) Haloperidol Selectively Remodels Striatal
651 Indirect Pathway Circuits. *Neuropsychopharmacology* 42: 963-973.
- 652 Shansky RM, Woolley CS (2016) Considering Sex as a Biological Variable Will Be Valuable for
653 Neuroscience Research. *J Neurosci* 36: 11817-11822.
- 654 Shuen JA, Chen M, Gloss B, Calakos N (2008) *Drd1a*-tdTomato BAC transgenic mice for
655 simultaneous visualization of medium spiny neurons in the direct and indirect pathways
656 of the basal ganglia. *J Neurosci* 28: 2681-2685.
- 657 Tallaksen-Greene SJ, Albin RL (1996) Splice variants of glutamate receptor subunits 2 and 3 in
658 striatal projection neurons. *Neuroscience* 75: 1057-1064.
- 659 Tansey EM, Arbuthnott GW, Fink G, Whale D (1983) Oestradiol-17 beta increases the firing
660 rate of antidromically identified neurones of the rat neostriatum. *Neuroendocrinology* 37:
661 106-110.
- 662 Tepper JM, Sharpe NA, Koos TZ, Trent F (1998) Postnatal development of the rat neostriatum:
663 electrophysiological, light- and electron-microscopic studies. *Dev Neurosci* 20: 125-145.
- 664 Thibault D, Loustalot F, Fortin GM, Bourque MJ, Trudeau LE (2013) Evaluation of D1 and D2
665 dopamine receptor segregation in the developing striatum using BAC transgenic mice.
666 *PLoS One* 8: e67219.
- 667 Ting JT, Feng G (2014) Recombineering strategies for developing next generation BAC
668 transgenic tools for optogenetics and beyond. *Front Behav Neurosci* 8: 111.
- 669 Tozzi A, de Iure A, Tantucci M, Durante V, Quiroga-Varela A, Giampa C, Di Mauro M,
670 Mazzocchi P, Costa C, Di Filippo M, Grassi S, Pettorossi VE, Calabresi P (2015)
671 Endogenous 17beta-estradiol is required for activity-dependent long-term potentiation in
672 the striatum: interaction with the dopaminergic system. *Front Cell Neurosci* 9: doi:
673 10.3389/fncel.2015.00192.
- 674 Uryu K, Butler AK, Chesselet MF (1999) Synaptogenesis and ultrastructural localization of the
675 polysialylated neural cell adhesion molecule in the developing striatum. *J Comp Neurol*
676 405: 216-232.

- 677 Valjent E, Bertran-Gonzalez J, Herve D, Fisone G, Girault JA (2009) Looking BAC at striatal
678 signaling: cell-specific analysis in new transgenic mice. *Trends Neurosci* 32: 538-547.
- 679 Venance L, Glowinski J (2003) Heterogeneity of spike frequency adaptation among medium
680 spiny neurones from the rat striatum. *Neuroscience* 122: 77-92.
- 681 Villalon Landeros R, Morisseau C, Yoo HJ, Fu SH, Hammock BD, Trainor BC (2012) Corncob
682 bedding alters the effects of estrogens on aggressive behavior and reduces estrogen
683 receptor-alpha expression in the brain. *Endocrinology* 153: 949-953.
- 684 Vorobjev VS, Sharonova IN, Haas HL, Sergeeva OA (2000) Differential modulation of AMPA
685 receptors by cyclothiazide in two types of striatal neurons. *Eur J Neurosci* 12: 2871-2880.
- 686 Will TR, Proano SB, Thomas AM, Kunz LM, Thompson KC, Ginnari LA, Jones CH, Lucas SC,
687 Reavis EM, Dorris DM, Meitzen J (2017) Problems and Progress regarding Sex Bias and
688 Omission in Neuroscience Research. *eNeuro* 4: pii: ENEURO.0278-0217.2017.
- 689 Willett JA, Johnson AG, Vogel AR, Patisaul HB, McGraw LA, Meitzen J (2018) Nucleus
690 accumbens core medium spiny neuron electrophysiological properties and partner
691 preference behavior in the adult male prairie vole, *Microtus ochrogaster*. *J Neurophysiol*
692 119: 1576-1588.
- 693 Willett JA, Will TR, Hauser CA, Dorris DM, Cao J, Meitzen J (2016) No evidence for sex
694 differences in the electrophysiological properties and excitatory synaptic input onto
695 nucleus accumbens shell medium spiny neurons. *eNeuro* 3: pii: ENEURO.0147-
696 0115.2016.
- 697 Wissman AM, McCollum AF, Huang GZ, Nikrodhanond AA, Woolley CS (2011) Sex
698 differences and effects of cocaine on excitatory synapses in the nucleus accumbens.
699 *Neuropharmacology* 61: 217-227.
- 700 Wong JE, Cao J, Dorris DM, Meitzen J (2016) Genetic sex and the volumes of the caudate-
701 putamen, nucleus accumbens core and shell: original data and a review. *Brain Struct*
702 *Funct* 221: 4257-4267.
- 703 Yoest KE, Quigley JA, Becker JB (2018) Rapid effects of ovarian hormones in dorsal striatum
704 and nucleus accumbens. *Horm Behav*: [Epub ahead of Print].
- 705 Young E, Korszun A (2010) Sex, trauma, stress hormones and depression. *Mol Psychiatry* 15:
706 23-28.
- 707 Young JW, Jentsch JD, Bussey TJ, Wallace TL, Hutcheson DM (2013) Consideration of species
708 differences in developing novel molecules as cognition enhancers. *Neurosci Biobehav*
709 *Rev* 37: 2181-2193.
- 710 Zurkovsky L, Brown SL, Boyd SE, Fell JA, Korol DL (2007) Estrogen modulates learning in
711 female rats by acting directly at distinct memory systems. *Neuroscience* 144: 26-37.

712

713

714 **Figure Legends**

715 **Figure 1.** Whole-cell patch clamped medium spiny neuron (MSNs) location in the caudate-
716 putamen of female and male Drd1a-tdTomato line 6 BAC transgenic mice. “Drd1a” males and
717 females represent recordings from fluorescently-labeled Drd1a-positive MSNs. “Drd2 ” males
718 and females represent recordings from non-fluorescently labeled MSNs. Acronyms: LV, lateral
719 ventricle; AC, anterior commissure; ACB, nucleus accumbens.

720 **Figure 2.** Action potential rheobase, threshold, and width vary by MSN subtype. A) Voltage
721 response of male and female Drd1a and Drd2 MSN subtypes to a depolarizing rheobase current
722 injection. B) Resting membrane potential exhibited greater diversity in male Drd1A MSNs. C)
723 Action potential rheobase is increased in Drd1a MSNs compared to Drd2 MSNs. D) Action
724 potential threshold is depolarized in Drd1a MSNs compared to Drd2 MSNs, and interacts with
725 sex. E) Action potential width is longer in Drd1a MSNs compared to Drd2 MSNs, and interacts
726 with sex. Acronyms: AP, action potential; *, $P<0.05$; **, $P<0.01$.

727 **Figure 3.** Action potential firing rates evoked by depolarizing current injections vary by MSN
728 subtype. A) Voltage response of male and female Drd1a and Drd2 MSN subtypes to a
729 depolarizing post-rheobase current injection. B) Drd1a MSNs exhibited decreased action
730 potential firing rates evoked by depolarizing current injections compared to Drd2 MSNs. C) The
731 slope of the evoked action potential to depolarizing current injection curve (FI slope) differed by
732 MSN subtype, with Drd2 MSNs exhibiting increased excitability compared to Drd1a MSNs.
733 Acronyms: FI Slope: slope of the evoked action potential to depolarizing current injection curve;
734 *, $P<0.05$; **, $P<0.01$; ****, $P<0.0001$.

735 **Figure 4.** Input resistance varies by MSN subtype. A) Voltage response of male and female
736 Drd1a and Drd2 MSN subtypes to a series of increasingly negative current injections (-0.01 nA
737 current steps). B) Injected negative current to steady-stage voltage deflection curve (IV curve).
738 Legend: red solid circles with red line: Drd1a males; black solid circles with black line: Drd2
739 males; red open circles with red line: Drd1a females; black open circles with black line: Drd2
740 females. C) Input resistance in the linear range is moderately decreased in Drd1a MSNs
741 compared to Drd2 MSNs. D) Input resistance in the rectified range does not differ between
742 subtypes. Acronyms: *, $P<0.05$.

743 **Figure 5.** mEPSC properties vary by MSN subtype. A) mEPSCs recorded from male and female
744 Drd1a and Drd2 MSN subtypes. MSNs were voltage clamped at -70 mV and mEPSCs were
745 recorded in the presence of tetrodotoxin (TTX) and picrotoxin (PTX) to block voltage-gated
746 sodium channels and GABAergic synaptic activity, respectively. B) mEPSC amplitude was
747 increased in Drd1a MSNs compared to Drd2 MSNs. C) mEPSC decay did not differ by subtype
748 or sex. D) mEPSC frequency did not differ by subtype or sex. Acronyms: mEPSC, miniature
749 excitatory postsynaptic current; **, $P<0.01$; ***, $P<0.001$.

750

751

752 **Tables (2)**753 **Table 1.** Drd1a and Drd2 Caudate-putamen Medium Spiny Neuron Properties Compared Across
754 Studies.

Property	Kreitzer and Malenka, 2007 [@]	Gertler et al., 2008	Cepeda et al., 2008	Ade et al., 2008 [%]	Chan et al., 2012	Planert et al., 2013	Planert et al., 2013	Goodliffe et al., 2018	Current study, 2019
Animal	Mice	Mice	Mice	Mice	Mice	Mice	Rats	Mice	Mice
MSN Subtype Identification	M4- or D2-eGFP BAC transgenic mice	D1 and D2 receptor-eGFP BAC transgenic mice on an FVB background	D1 and D2 receptor-eGFP BAC transgenic mice	D1 and D2 receptor-eGFP BAC transgenic mice on a C57BL/6J background	D1 and D2 receptor-eGFP BAC transgenic mice on either a FVB/NJ or C57BL/6J background	D1 receptor-eGFP BAC transgenic mice	Retrograde labeling of striatonigral MSNs	D1 and D2 receptor-eGFP BAC transgenic mice on a C57BL/6J background	B6 Cg-Tg (Drd1a-tdTomato) ⁶ Calak/J hemizygous mice on a C57BL/6J background
Animal Age	P20-25	P17-70	P39.7 ± 1.6	P16-25	P21-35	P15, 21-32	P14-19	~P365	P17-22
Animal Sex	Not reported	Not reported	Not reported	Male and female data pooled regardless of sex	Male	Not reported	Not reported	Male and Female data pooled regardless of sex	Male and Female data analyzed by sex
Resting Membrane Potential	D1=D2	D1<D2	---	D1=D2	---	D1=D2	D1=D2	D1=D2	D1=D2
Rheobase	---	D1>D2	---	---	---	D1>D2 [#]	D1>D2	D1>D2	D1>D2
AP Threshold	---	D1=D2	D1>D2	---	---	D1=D2	D1=D2	D1>D2	D1>D2
AP Amplitude	---	---	D1=D2	---	---	---	---	D1=D2	D1=D2
AP Amplitude change from first to second AP	---	---	---	---	---	D1=D2	D1>D2	---	---
AP width	---	---	D1=D2	---	---	D1=D2	D1=D2	---	D1>D2
AHP Peak	---	---	D1=D2	---	---	---	---	---	D1=D2
AHP Time to Peak	---	---	---	---	---	---	---	---	D1=D2
Frequency of evoked action potentials/FI slope	D1<D2	D1<D2	---	D1<D2	D1<D2	D1=D2	D1=D2	---	D1<D2
Linear Range Input Resistance	D1=D2	D1<D2	D1=D2	D1=D2	---	D1=D2	D1<D2	D1=D2	D1<D2
Rectified	---	---	---	---	---	D1=D2	D1=D2	---	D1=D2

Range Input Resistance									
% Inward Rectification	---	---	---	---	---	---	---	---	D1=D2
Time Constant of the Membrane	---	D1>D2	D1=D2	---	---	D1=D2	D1<D2	D1<D2	D1=D2
Capacitance	---	D1>D2	D1=D2	---	---	---	---	---	D1=D2
sEPSC Frequency	---	---	D1<D2	---	---	---	---	---	---
sEPSC Amplitude	---	---	D1=D2	---	---	---	---	---	---
sEPSC Kinetics	---	---	D1=D2	---	---	---	---	---	---
mEPSC Frequency	D1<D2	---	D1<D2*	---	---	---	---	D1=D2	D1=D2
mEPSC Amplitude	D1=D2	---	D1=D2	---	---	---	---	D1=D2	D1<D2
mEPSC Decay	D1=D2	---	D1=D2	---	---	---	---	---	D1=D2
mEPSC Rise Time	---	---	D1<D2	---	---	---	---	---	D1=D2
s/mIPSC Frequency	---	---	---	D1=D2	---	---	---	---	---
s/mIPSC Amplitude	---	---	---	D1=D2	---	---	---	---	---
s/mIPSC Decay	---	---	---	D1=D2	---	---	---	---	---
s/mIPSC Rise Time	---	---	---	D1=D2	---	---	---	---	---
Probability of occurrence of spontaneous membrane depolarization after GABA _A blockade	---	---	D1<D2	---	---	---	---	---	---
Paired-Pulse Ratio	D1>D2	---	D1<D2	---	---	---	---	---	---
AMPA-induced current amplitude	---	---	D1>D2	---	---	---	---	---	---
NMDA/AMPA Ratio	D1<D2	---	---	---	---	---	---	---	---
Endocannabinoid-mediated LTD	D1<D2	---	---	---	---	---	---	---	---
Tonic GABA _A current and sensitivity to GABA _A current	---	---	D1<D2	D1<D2	---	---	---	---	---

755 Only caudate-putamen MSN subtype electrophysiology studies in acute brain slice preparation experiments independent of variables such as
 756 dopamine depletion and psychostimulant exposure are included. This criteria *a priori* excludes studies that analyzed MSN subtype
 757 electrophysiological properties but did not directly compare D1 and D2 subtype groups, for example (Day et al., 2006; Ade et al., 2011), or were
 758 performed in regions such as the nucleus accumbens, for example (Ma et al., 2012; Cao et al., 2018). Acronyms: ---, did not measure; AP, action
 759 potential; AHP, afterhyperpolarization, FI: Frequency of evoked spikes to injected depolarization current; s/mEPSC, spontaneous/miniature
 760 excitatory post-synaptic current. IPSC, inhibitory post-synaptic current; LTD: long term depression. *This finding significant in some but not all
 761 analyses within this study. #Planert and colleagues assessed rheobase using multiple analyses. The conclusion of all analyses was similar and is

762 thus condensed here. [@]The use of M4 eGFP labeling as equivalent to the D1 MSN subtype has been cautioned (Cepeda et al., 2008). [%]A number
763 of studies from Vicini and colleagues have investigated GABA conductance between MSN subtypes; here we feature the initial report.

764

765

766 **Table 2.** Electrophysiological Properties of Male and Female Drd1a and Drd2 Mouse Caudate-
 767 putamen Medium Spiny Neurons

Property	Drd1a	Drd2	Statistics (<i>F</i> , <i>P</i>)
Resting Potential (mV)	Male: -90.9 ± 1.2^a Female: $-87.5 \pm 0.7^{a,b}$	Male: -85.0 ± 1.8^b Female: $-89.0 \pm 1.2^{a,b}$	Interaction: $F_{(1,82)}=8.7$; $P=0.004$ Sex: $F_{(1,82)}=0.1$; $P=0.75$ Subtype: $F_{(1,82)}=2.8$; $P=0.10$ Post-hoc: Tukey's
Rheobase (nA)	Male: 0.16 ± 0.01^a Female: 0.16 ± 0.01^a	Male: 0.10 ± 0.02^b Female: $0.12 \pm 0.02^{a,b}$	Interaction: $F_{(1,82)}=0.4$; $P=0.52$ Sex: $F_{(1,82)}=0.4$; $P=0.54$ Subtype: $F_{(1,82)}=12.3$; $P=0.0007$ Post-hoc: Tukey's
AP Threshold (mV)	Male: $-58.3 \pm 1.0^{a,b}$ Female: -54.6 ± 1.2^a	Male: $-58.6 \pm 0.7^{a,b}$ Female: -62.6 ± 2.9^b	Interaction: $F_{(1,81)}=7.2$; $P=0.0087$ Sex: $F_{(1,81)}=0.01$; $P=0.90$ Subtype: $F_{(1,81)}=8.0$; $P=0.0058$ Post-hoc: Tukey's
AP Amplitude (mV)	Male: 68.8 ± 2.1 Female: 69.5 ± 2.9	Male: 69.3 ± 2.8 Female: 79.1 ± 3.1	Interaction: $F_{(1,81)}=2.3$; $P=0.13$ Sex: $F_{(1,81)}=3.1$; $P=0.08$ Subtype: $F_{(1,81)}=3.0$; $P=0.09$
AP width at half-peak (ms)	Male: 1.63 ± 0.05^a Female: $1.45 \pm 0.05^{a,b}$	Male: 1.31 ± 0.06^b Female: $1.43 \pm 0.15^{a,b}$	Interaction: $F_{(1,80)}=4.7$; $P=0.0339$ Sex: $F_{(1,80)}=0.1$; $P=0.7052$ Subtype: $F_{(1,80)}=5.3$; $P=0.0234$ Post-hoc: Tukey's
AHP Peak (mV)	Male: -8.9 ± 0.4 Female: -11.0 ± 0.7	Male: -9.8 ± 0.8 Female: -9.2 ± 0.7	Interaction: $F_{(1,80)}=3.5$; $P=0.0654$ Sex: $F_{(1,80)}=0.8$; $P=0.37$ Subtype: $F_{(1,80)}=0.2$; $P=0.69$
AHP Time to Peak (ms)	Male: 32.2 ± 1.3 Female: 26.3 ± 1.6	Male: 31.8 ± 3.4 Female: 32.5 ± 3.2	Interaction: $F_{(1,81)}=2.1$; $P=0.15$ Sex: $F_{(1,81)}=1.4$; $P=0.24$ Subtype: $F_{(1,81)}=1.6$; $P=0.21$
FI Slope (Hz/nA)	Male: 192.5 ± 10.4^a Female: 164.0 ± 12.8^a	Male: 278.7 ± 28.9^b Female: 242.0 ± 23.0^b	Interaction: $F_{(1,81)}=0.1$; $P=0.82$ Sex: $F_{(1,81)}=3.4$; $P=0.0708$ Subtype: $F_{(1,81)}=21.2$; $P<0.0001$ Post-hoc: Tukey's
Linear Range Input Resistance (M Ω)	Male: 102.1 ± 5.8^a Female: 93.6 ± 6.6^a	Male: 141.0 ± 19.2^b Female: $109.8 \pm 18.3^{a,b}$	Interaction: $F_{(1,78)}=1.1$; $P=0.30$ Sex: $F_{(1,78)}=2.9$; $P=0.09$ Subtype: $F_{(1,78)}=6.3$; $P=0.0138$ Post-hoc: Tukey's
Rectified Range Input Resistance (M Ω)	Male: 83.4 ± 4.7 Female: 83.9 ± 8.6	Male: 112.0 ± 17.7 Female: 83.1 ± 11.7	Interaction: $F_{(1,79)}=2.0$; $P=0.16$ Sex: $F_{(1,79)}=1.9$; $P=0.17$ Subtype: $F_{(1,79)}=1.8$; $P=0.18$
% Inward Rectification (%)	Male: 82.3 ± 1.3 Female: 81.0 ± 1.8	Male: 80.8 ± 4.3 Female: 79.2 ± 3.3	Interaction: $F_{(1,79)}=0.0$; $P=0.93$ Sex: $F_{(1,79)}=0.3$; $P=0.57$ Subtype: $F_{(1,79)}=0.4$; $P=0.52$
Time Constant of the Membrane (ms)	Male: 10.3 ± 0.8 Female: 19.6 ± 1.2	Male: 14.6 ± 3.2 Female: 9.9 ± 1.9	Interaction: $F_{(1,82)}=2.9$; $P=0.09$ Sex: $F_{(1,82)}=1.2$; $P=0.28$ Subtype: $F_{(1,82)}=1.6$; $P=0.20$
Capacitance (pF)	Male: 109.6 ± 10.0 Female: 99.0 ± 7.0	Male: 94.4 ± 11.2 Female: 91.2 ± 8.5	Interaction: $F_{(1,78)}=0.1$; $P=0.74$ Sex: $F_{(1,78)}=0.4$; $P=0.55$ Subtype: $F_{(1,78)}=1.0$; $P=0.31$
mEPSC Frequency (Hz)	Male: 1.9 ± 0.2 Female: 1.9 ± 0.2	Male: 2.0 ± 0.5 Female: 1.4 ± 0.4	Interaction: $F_{(1,47)}=0.9$; $P=0.33$ Sex: $F_{(1,47)}=1.2$; $P=0.29$ Subtype: $F_{(1,47)}=0.3$; $P=0.58$
mEPSC Amplitude (pA)	Male: 15.9 ± 0.4^a Female: 15.2 ± 0.6^a	Male: $17.7 \pm 1.1^{a,b}$ Female: 20.7 ± 1.5^b	Interaction: $F_{(1,47)}=5.2$; $P=0.0270$ Sex: $F_{(1,47)}=2.1$; $P=0.1498$ Subtype: $F_{(1,47)}=20.4$; $P<0.0001$ Post-hoc: Tukey's
mEPSC Decay (ms)	Male: 1.9 ± 0.2 Female: 1.9 ± 0.2	Male: 2.0 ± 0.5 Female: 1.4 ± 0.4	Interaction: $F_{(1,47)}=2.6$; $P=0.11$ Sex: $F_{(1,47)}=0.1$; $P=0.76$ Subtype: $F_{(1,47)}=0.0$; $P=0.95$

768 Values are mean \pm SEM. Bold font indicates statistical significance. Different superscript letters denote significant
769 differences detected by a Tukey's post-hoc test. Abbreviations: MSN, medium spiny neuron; AP, action potential;
770 AHP, afterhyperpolarization; FI, Frequency of evoked spikes to injected depolarization current; mEPSC, miniature
771 excitatory post-synaptic current.

Figure 1

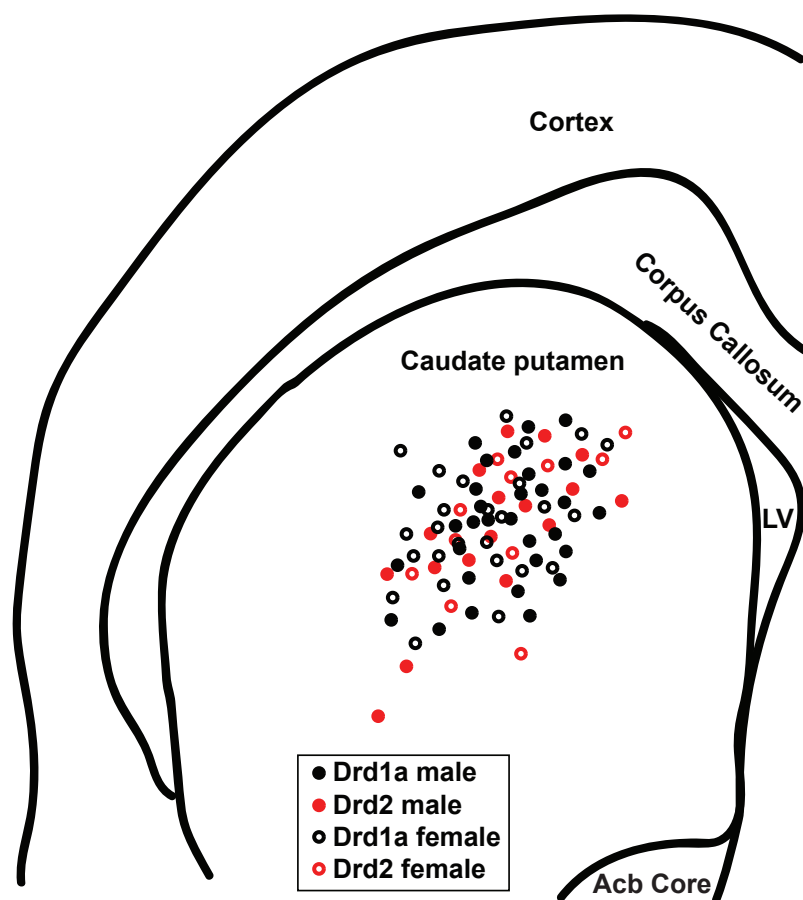
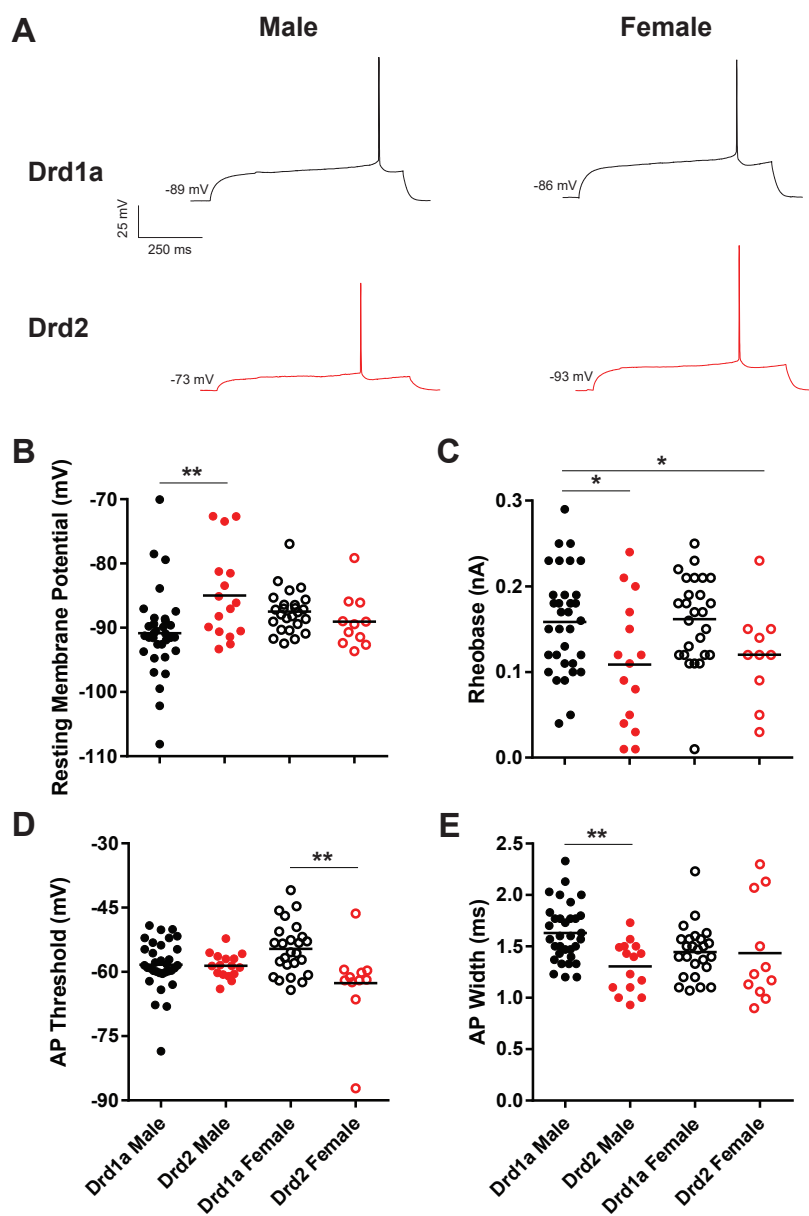


Figure 2



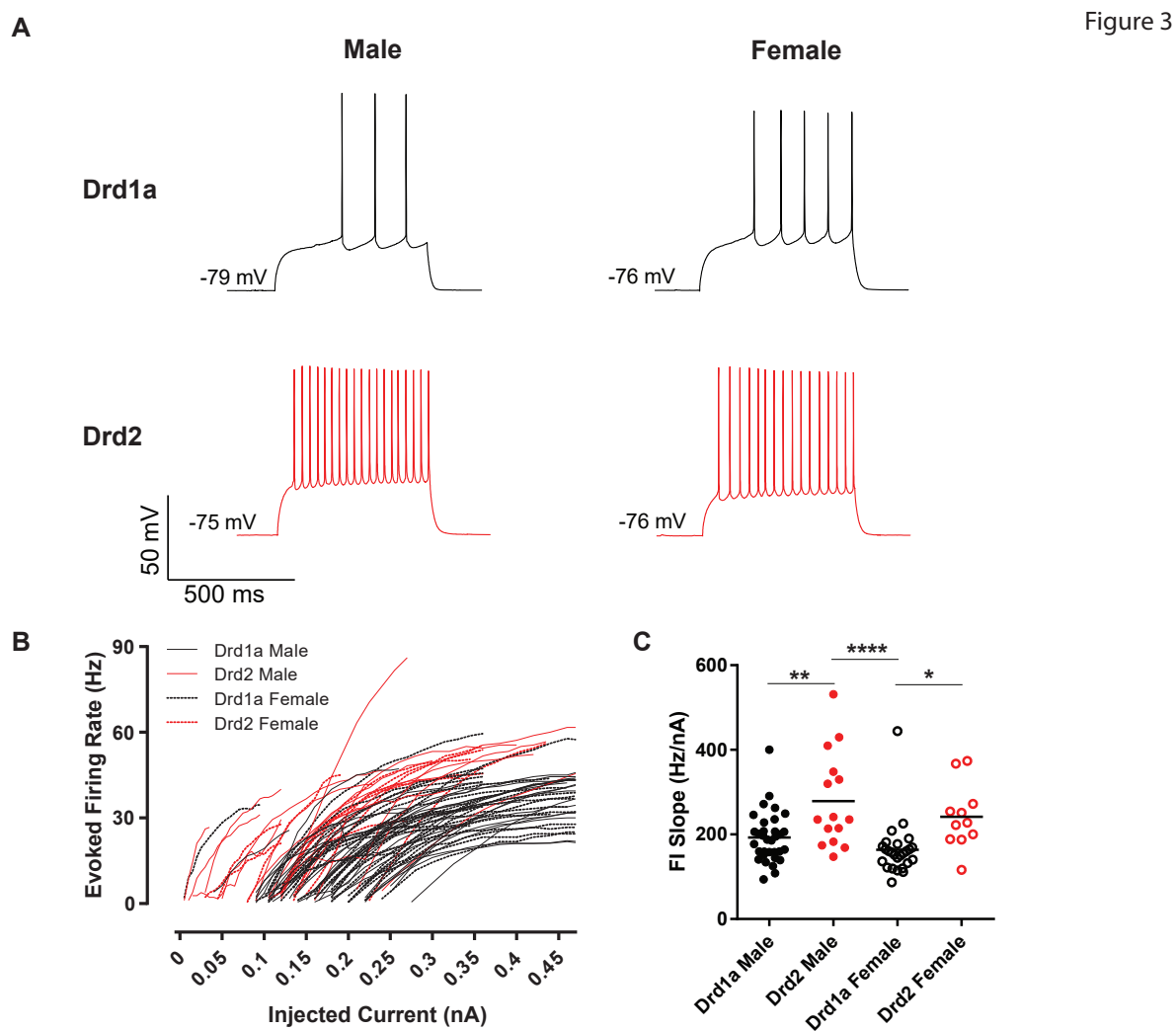


Figure 4

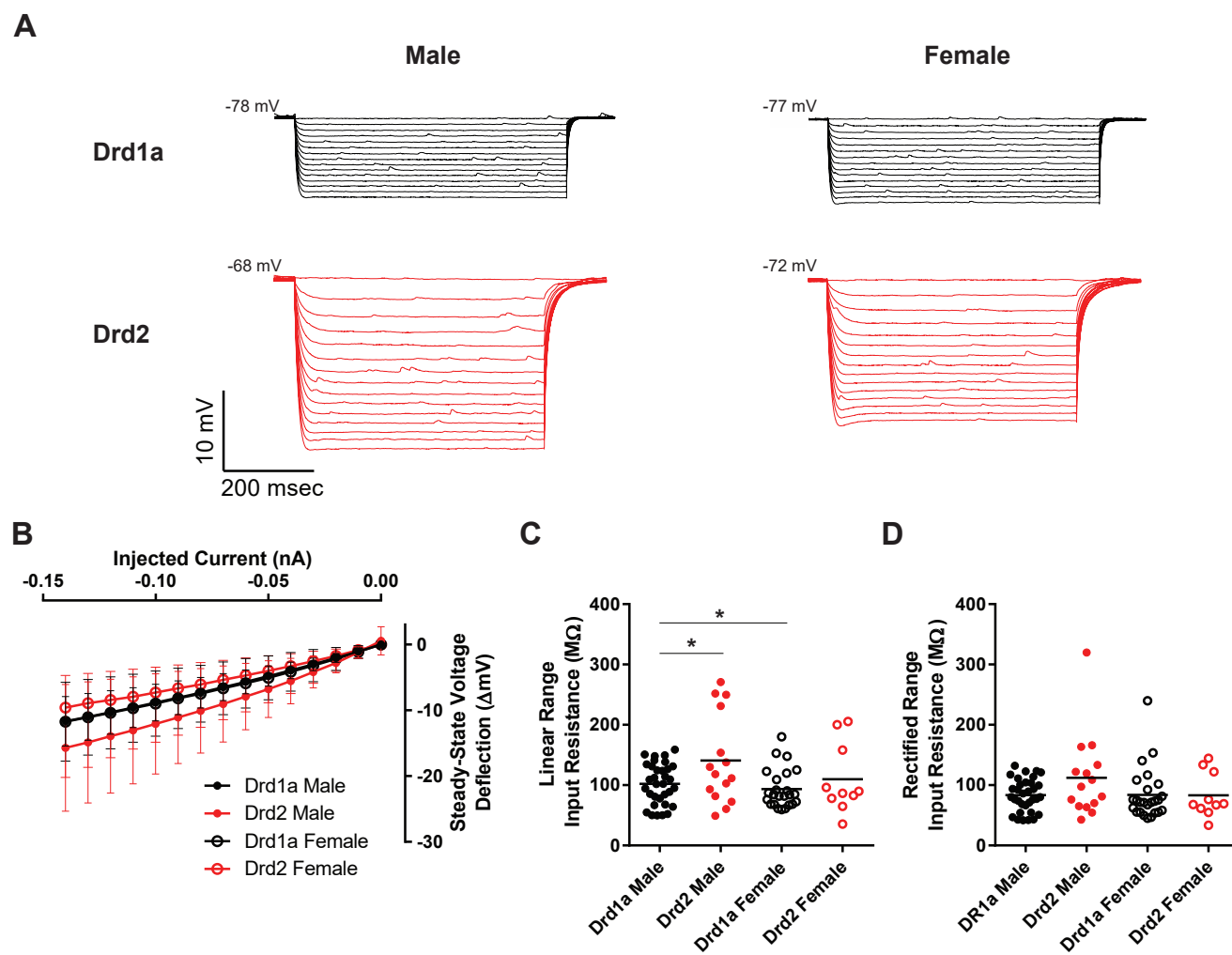


Figure 5

